



Noise and the PSTH Response to Current Transients: II. Integrate-and-Fire Model with Slow Recovery and Application to Motoneuron Data*

A. HERRMANN** AND W. GERSTNER

*Laboratory of Computational Neuroscience, Swiss Federal Institute of Technology Lausanne,
CH-1015 Lausanne EPFL, Switzerland*

alix.hermann@evid.ch

wulfram.gerstner@epfl.ch

Received December 29, 1999; Revised November 25, 2000; Accepted June 19, 2001

Action Editor: John Miller

Abstract. A generalized version of the integrate-and-fire model is presented that qualitatively reproduces firing rates and membrane trajectories of motoneurons. The description is based on the spike-response model and includes three different time constants: the passive membrane time constant, a recovery time of the input conductance after each spike, and a time constant of the spike afterpotential. The effect of stochastic background input on the peristimulus time histogram (PSTH) response to spike input is calculated analytically. Model results are compared with the experimental data of Poliakov et al. (1996). The linearized theory shows that the PSTH response to an input spike is proportional to a filtered version of the postsynaptic potential generated by the input spike. The shape of the filter depends on the background activity. The full nonlinear theory is in close agreement with simulated PSTH data.

Keywords: PSTH, synaptic noise, spike-response model, motoneuron

1. Introduction

What is the typical response of a neuron to an input spike? In the companion paper (Herrmann and Gerstner, 2000), we developed a theoretical framework for studying the effect of stochastic background input (modeled as diffusive noise) on the peristimulus time histogram (PSTH). The theory was illustrated using a standard integrate-and-fire neuron. A major shortcoming of the integrate-fire model is that it has only one time constant. Especially for tonic firing, it produces an unrealistic membrane trajectory if the experimen-

tally measured passive time constant is used because the recovery processes during refractoriness following an action potential are not modeled at all. However, experimental studies of the effect of noise on the PSTH are generally conducted on tonically firing neurons (Fetz and Gustafsson, 1983; Poliakov et al., 1996, 1997). The goal of this paper is to show that the effect of noise on the PSTH demonstrated for the integrate-and-fire neuron in the companion paper can also be obtained using a model with a more realistic membrane trajectory, but without incorporating further biological details such as specific ionic conductances or adaptation.

In Poliakov et al. (1996, 1997), PSTH responses to Poisson-distributed trains of current pulses were recorded. The pulses were injected into the soma of rat hypoglossal motoneurons during repetitive discharge. The time course of the pulses was chosen to mimic

*To read Part I of this article please refer to Volume 11, Number 2, pages 135–151.

**Current address: Ecole d'Ingénieurs de l'Etat de Vaud (EIVD), Yverdon-les-Bains, Switzerland.

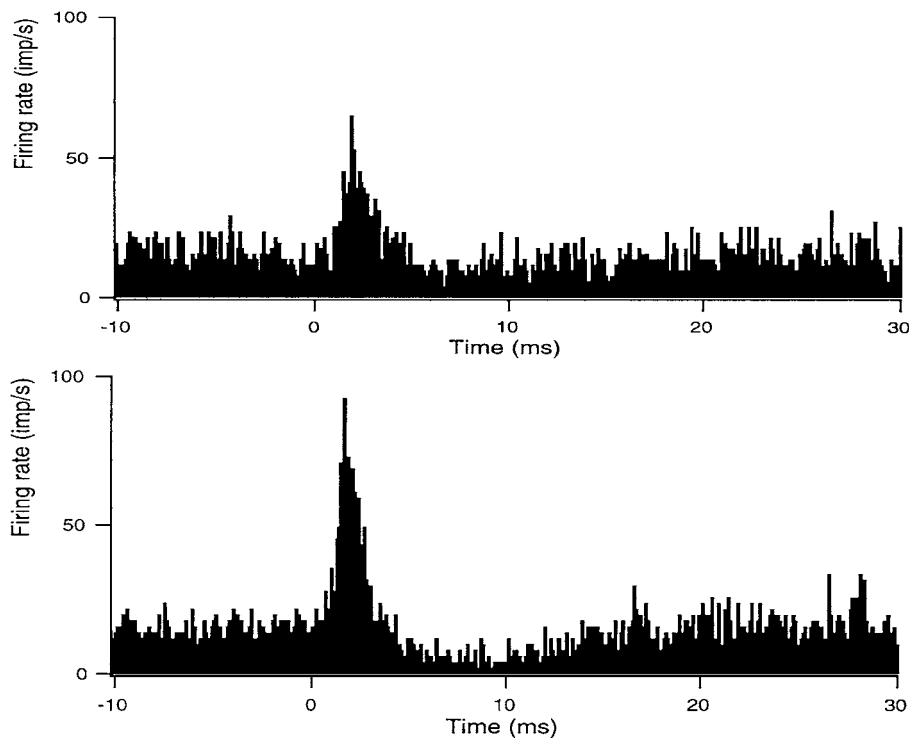


Figure 1. Effect of noise on the PSTH response of a rat hypoglossal motoneuron. A Poisson train of excitatory alpha-shaped current pulses of amplitude 0.2 nA was injected into the soma of a rat hypoglossal motoneuron, superimposed on a long 1 nA current step inducing repetitive firing. In the “high” noise condition, this input was combined with an additional noise waveform. **A:** PSTH “high” noise (noise power level $30 \text{ nA}^2 \mu\text{s}$). **B:** “Low” noise (courtesy of M. Binder; data from Poliakov et al., 1996).

postsynaptic currents generated by presynaptic spike arrival. PSTHs of motoneuron discharge occurrences were compiled when the pulse trains were delivered either with or without additional current noise which simulated noisy background input. Figure 1 shows examples of responses from a rat motoneuron taken from the work of Poliakov et al. (1996). The effect of adding noise can be seen clearly: the low-noise peak is followed by a marked trough, whereas the high-noise PSTH has a reduced amplitude and a much smaller trough. We show in this article that simulations of our motoneuron model produce low- and high-noise PSTHs similar to the experimental ones. Furthermore, the PSTH responses can be predicted analytically. Figure 2 shows PSTHs produced by simulations of our model (thin, stepped lines) and responses predicted from the theory (thick solid and dashed lines; see figure caption for details) using the same current pulses and noise levels as in the experiments. The neuron parameters we used were chosen ad hoc from the range of values described as typical by Poliakov et al. (1996) and are probably not the same as those of the motoneu-

ron in Fig. 1. Consequently, the PSTH peak amplitudes and timecourses are somewhat different. Nevertheless, it is clear that the effect of noise is the same: in both the simulations and the experiments, current noise with a power level of $30 \text{ nA}^2 \mu\text{s}$ reduces the amplitude of the low-noise peak by about half.

2. Methods

In order to obtain a realistic membrane trajectory in a tonically firing neuron (subjected to suprathreshold stimulation), we use the spike-response model framework summarized below.

2.1. General Spike-Response Model

The spike-response model (Gerstner, 1995, 2000, 2001) consists of a threshold ϑ , a refractory function η , and a response kernel ε describing the response of the neuron to an external current input $I(t)$.

The refractory function $\eta(t - \hat{t})$ generates the afterhyperpotential following a spike at time \hat{t} . The kernel

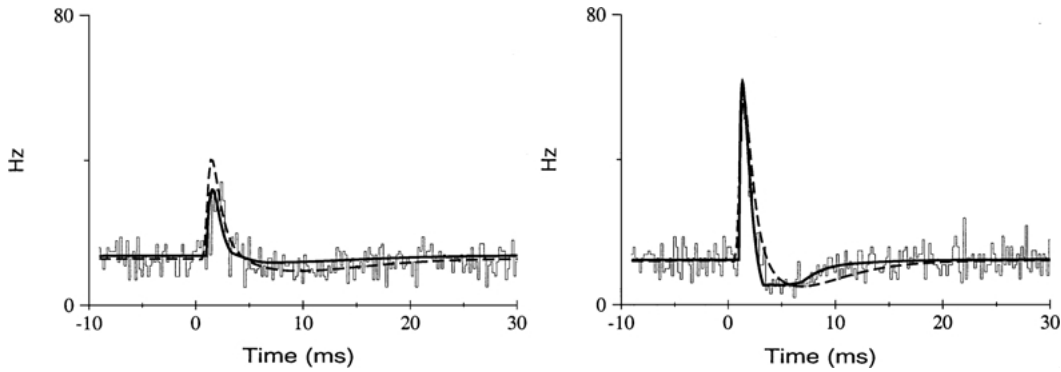


Figure 2. PSTH response to an alpha-shaped input pulse (rise time 0.5 ms) at $t = 0$. All responses incorporate a 1 ms delay introduced to simulate the time taken for spike initiation and spike detection in real neurons (Poliakov et al., 1996). Thin stepped lines, simulation results equivalent to 5,000 trials (time step 0.1 ms averaged to 0.2 ms). Thick dashed curves, theoretical predictions using the linear approximation. Thick solid curves, theoretical predictions using the full escape noise model; a discontinuity visible at the beginning of the trough stems from the $H[u']$ term in the escape rate, Eq. (7). Left, “high” noise (noise power level $30 \text{ nA}^2 \mu\text{s}$). Right, “low” noise (noise power level $5 \text{ nA}^2 \mu\text{s}$).

$\varepsilon(t - \hat{t}, s)$ describes the response of the membrane to small fluctuations; the $t - \hat{t}$ dependence allows spike-time dependent conductance changes to be represented. The net input potential

$$h(t | \hat{t}) = \int_0^\infty \varepsilon(t - \hat{t}, s) I(t - s) ds \quad (1)$$

integrates the current input $I(t)$. The resulting membrane potential $u(t)$ is the sum of the (negative) refractory potential and the net input potential,

$$u(t) = \eta(t - \hat{t}) + h(t | \hat{t}) \quad (2)$$

where \hat{t} is the last firing time of the neuron. When the membrane potential exceeds the threshold, a spike is emitted and the potential is reset by setting $\hat{t} = t$ in Eq. (2).

2.2. Neuron Model with Slow Recovery

A simple version of the spike-response model equivalent to the standard integrate-and-fire model was studied in the companion paper (Herrmann and Gerstner, 2000). The standard integrate-and-fire model is characterized by a single time constant—i.e., the passive membrane time constant τ_m . By adding two further time constants we obtain a model that behaves more reasonably when physiologically plausible parameter values are used but that can still be reduced to the standard integrate-and-fire model in a certain limit.

In order to compare with motoneuron experiments, we want a neuron model that retains the general features of a tonically firing motoneuron in the primary range,

while remaining as simple as possible. The key features of the membrane potential dynamics to be preserved are: a parallel RC-circuit-like passive membrane response to small signals; a slow exponential return to the resting potential following a spike in the absence of further stimulation; and a roughly linear trajectory of membrane potential when approaching threshold during tonic firing.

To achieve this, we will use the spike-response model with the following kernels:

$$\eta(t - \hat{t}) = -\eta_0 e^{-\frac{(t-\hat{t})}{\tau_{\text{refr}}}} H(t - \hat{t}) \quad (3)$$

$$\varepsilon(t - \hat{t}, s) = \frac{R}{\tau_m} \left(1 - e^{-\frac{(t-\hat{t})}{\tau_{\text{rec}}}}\right) e^{-\frac{s}{\tau_m}} H(s) H(t - \hat{t} - s) \quad (4)$$

where τ_m is the effective passive membrane time constant (Bernander et al., 1991) (see also Section 4.2), R is the input resistance, τ_{refr} is the “refractory” time constant, τ_{rec} is the “response recovery” time constant, η_0 is a scale factor for the refractory function, and $H(\cdot)$ is the Heaviside step function with $H(x) = 0$ for $x \leq 0$ and $H(x) = 1$ for $x > 0$. Experimentally, the passive membrane time constant τ_m and input resistance R would be determined from the responses to small current pulses. The refractory function η describes the return of the membrane potential to baseline after an action potential. It is characterized by a slow time constant τ_{refr} . The parameters η_0 and τ_{refr} would be chosen to fit the membrane trajectory following a single spike, in the absence of any further current input after the action potential has been triggered (see Fig. 3). Thus τ_{refr} would normally be much longer than τ_m .

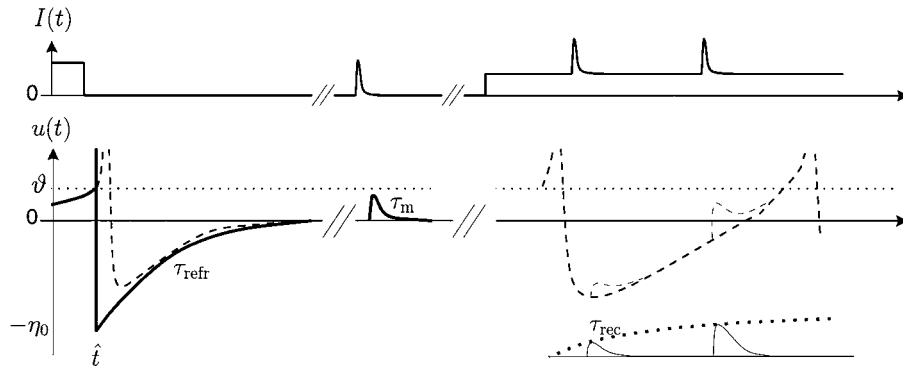


Figure 3. Determination of model time constants in a hypothetical experiment: $I(t)$, input current; $u(t)$, membrane potential. Dashed trace, measured trajectory; thick trace, fitted trajectory. At left, the refractory time constant τ_{refr} is measured by fitting an exponential to the membrane trajectory following a single spike, when the input is set to 0 immediately after the spike. Once the potential has reached its resting value, the membrane time constant τ_m is determined from the response to a small current pulse. At right, the response recovery time constant τ_{rec} is determined from the response to a pulse train applied during tonic firing. Immediately after the action potential, the responses have smaller amplitude; the response amplitude recovers with a time constant τ_{rec} (bottom).

For the ε -kernel we use a decaying exponential in s with time constant τ_m , modulated by the “recovery” factor $(1 - \exp[-(t - \hat{t})/\tau_{\text{rec}}])$. This mimics a spike-time dependent scaling of the input conductance;¹ τ_{rec} is expected to be longer than τ_m . In the simulations in this article, we use the same time constant as for the refractory function η —i.e. we take $\tau_{\text{refr}} = \tau_{\text{rec}} = 100$ ms. The remaining parameter values are listed in Table 1. For a constant current $I_0 = 1.0$ nA, this gives a membrane potential trajectory whose slope near threshold is 0.26 mV/ms; the mean interspike interval is $t_0 \approx 80$ ms. These values are similar to those reported for rat hypoglossal motoneurons (Poliakov et al., 1996).

The effect of the modulation of the input conductance on the response to small pulses is depicted in Fig. 4. Experimental support for a roughly exponential time course of the recovery of the input conductance of motoneurons can be found in Schwindt and Calvin (1973) and Powers and Binder (1996). The important effect of this extra factor is to lengthen the interspike interval during tonic firing relative to the standard integrate-and-fire model, as shown in Fig. 5.

To relate our model to the integrate-and-fire model, we can write out the membrane potential. Between

spikes, the deterministic membrane potential evolves according to

$$u(t) = \eta(t - \hat{t}) + \int_0^\infty \varepsilon(t - \hat{t}, s) I(t - s) ds$$

$$= -\eta_0 e^{-\frac{(t-\hat{t})}{\tau_{\text{refr}}}} H(t - \hat{t}) + \frac{R}{\tau_m} (1 - e^{-\frac{(t-\hat{t})}{\tau_{\text{rec}}}}) \int_0^{t-\hat{t}} e^{-\frac{s}{\tau_m}} I(t - s) ds. \quad (5)$$

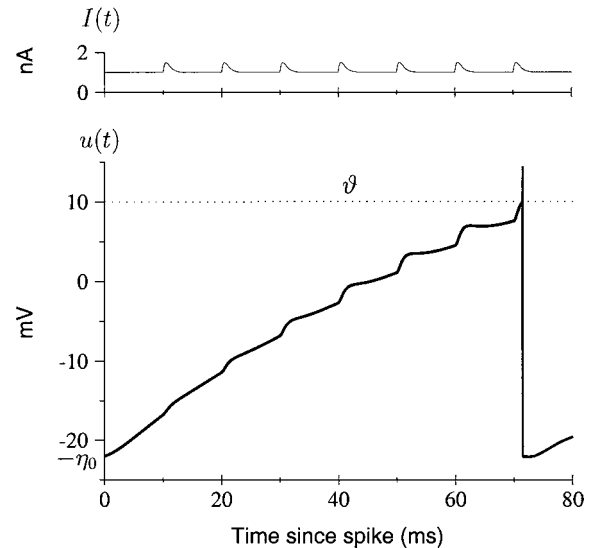


Figure 4. Effect of recovery time constant τ_{rec} . The membrane potential response (thick line) to an input pulse train (thin line) clearly shows that the response amplitude decreases as a function of the time since the last spike. Input pulses have rise time 0.5 ms, amplitude 0.5 nA.

Table 1. Parameter values used in the slow recovery model to simulate motoneurons.

R	ϑ	η_0	τ_m	τ_{rec}	τ_{refr}
36 M Ω	10 mV	22 mV	4 ms	100 ms	100 ms

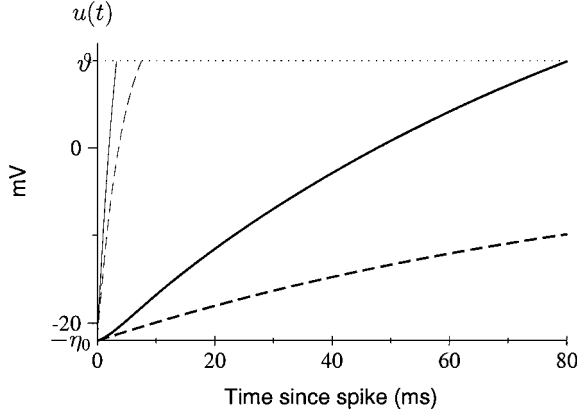


Figure 5. Lengthening of the ISI resulting from the conductance modulation term. Thick solid line, membrane trajectory following a spike using the model defined in Eq. (5) and the parameters indicated in the text, with constant input current $I_0 = 1$ nA. Thick dashed line, the trajectory for $I_0 = 0$ asymptotically approaches zero. (This trajectory is equal to the time course of the refractory function η). Thin dashed line, trajectory if the conductance modulation is removed ($\tau_{\text{rec}} = 0$, “instant recovery”). Thin solid line, trajectory of the integrate-and-fire reduction ($\tau_{\text{refr}} = \tau_m = 4$ ms).

After each spike, the new initial condition or “reset” is $u(\hat{t}) = \eta_0$. In the limit $\tau_{\text{rec}} \rightarrow 0$ (“instant recovery”), $(1 - \exp[-(t - \hat{t})/\tau_{\text{rec}}]) \rightarrow 1$; after taking the time derivative and setting $\tau_{\text{refr}} = \tau_m$ we recover the standard integrate-and-fire equation: $\tau_m u'(t) = -u(t) + RI(t)$.

A second reduction is possible that emphasizes the long time constants τ_{refr} and τ_{rec} . Let us define a recovery state variable, $r(t - \hat{t}) = \exp[-(t - \hat{t})/\tau_{\text{rec}}]$ and the free potential $h_{\text{free}}(t) = R/\tau_m \int_0^\infty \exp(-s/\tau_m) I(t - s) ds$. Taking the derivatives of Eq. (5), we arrive at the following set of three differential equations:

$$\begin{aligned} \tau_{\text{refr}} u'(t) &= -u(t) + h_{\text{free}}(t) \left[1 - \frac{\tau_{\text{refr}}}{\tau_{\text{rec}}} \right] \\ &\quad + [1 - r(t)] \frac{\tau_{\text{refr}}}{\tau_m} RI(t) \\ &\quad - r(t) h_{\text{free}}(t) \left[1 - \tau_{\text{refr}} \left(\frac{1}{\tau_m} + \frac{1}{\tau_{\text{rec}}} \right) \right] \\ \tau_{\text{rec}} r'(t) &= -r(t) \\ \tau_m h'_{\text{free}}(t) &= -h_{\text{free}}(t) + RI(t), \end{aligned} \quad (6)$$

with the reset conditions $r(\hat{t}) = 1$, $h_{\text{free}}(\hat{t}) = 0$ and $u(\hat{t}) = \eta_0$ as before. This defines a system in three variables: the variable with fast dynamics is h_{free} with time constant τ_m ; the slow variables r and u have respective time constants τ_{refr} and τ_{rec} . The system of differential

Eq. (6) is equivalent to Eq. (5) but leads to a faster numerical implementation.

2.3. Noise Model

To represent the effect of noisy background input, we use escape noise (Gerstner, 2000; Plesser and Gerstner, 2000). Rather than explicitly adding noise to the input current, we consider that the probability of spiking depends on the distance to threshold of the membrane potential. In this article we use the Gaussian ISI escape rate function motivated in Herrmann and Gerstner (2000), defined as

$$f(u - \vartheta) = 1.21 \left[\frac{1}{\tau} + 2u'H(u') \right] \frac{G(u - \vartheta, \sigma_u)}{\text{Erfc}\left(\frac{u - \vartheta}{\sqrt{2}\sigma_u}\right)}, \quad (7)$$

where $G(x, \sigma)$ is the Gaussian $(\sigma\sqrt{2\pi})^{-1} \exp[-x^2/(2\sigma^2)]$, $\text{Erfc}(x) = 1 - \text{Erf}(x)$ is the complementary error function, and $u' = (du/dt)$ evaluated at t . With this function and $u' = 0$, the probability of a spike increases as the potential approaches threshold from below; above threshold, it is asymptotically linear.

Using this formulation, the time-dependent hazard function (probability of spiking as a function of time since \hat{t}) is simply $\rho(t|\hat{t}) = f[u(t - \hat{t}), u'(t - \hat{t})]$ where u is given by Eq. (2). We can also determine the survivor function S_h for a given input h (i.e., the probability that a neuron does *not* fire between \hat{t} and t when h is applied), since the survivor function is related to the hazard function $\rho(t|\hat{t})$ (Perkel et al., 1967; Cox, 1962):

$$S_h(t|\hat{t}) = \exp\left[-\int_{\hat{t}}^t \rho(t'|\hat{t}) dt'\right]. \quad (8)$$

For constant input h_0 , the survivor function is denoted $S_0(t - \hat{t})$.

3. Results

Using the neuron model and noise model defined above, we apply the theory presented in the companion paper (Herrmann and Gerstner, 2000) to obtain an analytical prediction of the PSTH response to an input pulse. In the next section we apply the theory to the neuron model defined by Eq. (5). In Section 3.2 we compare our predictions with simulations.

3.1. Theoretical Results

In Herrmann and Gerstner (2000) we argue that the PSTH, expressed as a firing rate, is equivalent to the population-averaged activity $A(t)$ of a homogeneous, asynchronous population of neurons. Therefore, the theory of population dynamics for neurons with escape noise (Gerstner, 2000) can be applied by identifying the time course of the PSTH as $A(t)$. When a pulse $I(t) = I_0 + \Delta I(t)$ is applied, the activity undergoes a perturbation from its stationary state $A(t) = A_0 + \Delta A(t)$. In PSTH terms, A_0 is the baseline firing rate while $\Delta A(t)$ gives the time course of the peak following the applied pulse. The theory provides the means to calculate $A(t)$ numerically for a given input $I(t)$ based on the survivor function. In addition, the theory can be used to obtain a first-order approximation of $A(t)$, which directly relates the form of the peak $\Delta A(t)$ to the postsynaptic potential resulting from $I(t)$ via a noise-dependent linear filter.

The mean rate A_0 can be found as the inverse of the mean interval. In the noiseless case, the neuron fires periodically and the interval can be computed from Eq. (2) by setting $u = \vartheta$. With noise, the mean interval can be computed as the integral of the survivor function: $1/A_0 = \int_0^\infty S(s) ds$. Figure 6 shows gain (f - I) curves for the model neuron using the survivor function for the specific noise model defined above in Eq. (7). Above threshold, the response is essentially linear, similar to that of a motoneuron in the primary firing range. Adding noise shifts the response to the left and extends the response range downward.

The dynamics of the activity of a population can be computed if the distribution of firing intervals $P_h(t | \hat{t})$

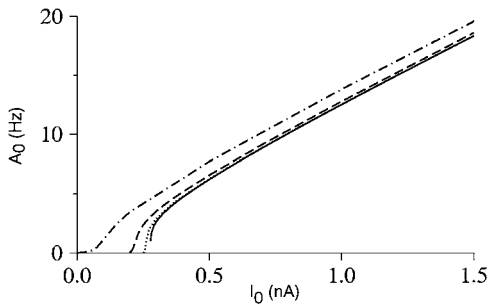


Figure 6. Gain (f - I) curves for the neuron model, parameter values as specified in the text. Solid: No noise. Dotted: noise level σ_u (defined in Eq. (7)) 0.1 mV; dashed: $\sigma_u = 1$ mV; dot-dashed, $\sigma_u = 10$ mV. The corresponding equivalent power levels for Gaussian current noise with 10 KHz bandwidth are 0.06, 6, and 600 nA² μ s, respectively.

is known (i.e., the probability of firing for each neuron at time t , given that the neuron last fired at time \hat{t} , when the net input potential is $h(t | \hat{t})$). The activity evolves according to Gerstner (2000)

$$A(t) = \int_{-\infty}^t P_h(t | \hat{t}) A(\hat{t}) d\hat{t}. \quad (9)$$

This nonlinear equation may be integrated numerically for certain choices of noise models and neuron models. For the integrate-and-fire neuron with slow recovery, we can apply the algorithm given in Herrmann and Gerstner (2000, app. A) with only slight modification.² However, the relation between the form of the PSTH and the input is not explicit in Eq. (9). As for the standard integrate-and-fire neuron studied in Herrmann and Gerstner (2000), we perform a first-order expansion of Eq. (9) to obtain an explicit relation between $\Delta A(t)$ and the “free” input potential h_{free} . In the Appendix it is shown that for the kernels of Eqs. (3) and (4), the form of the PSTH may be approximated using a linear filter:

$$\Delta A(t) = \int_{-\infty}^t d\hat{t} P_{h_0}(t | \hat{t}) \Delta A(\hat{t}) + A_0 \frac{d}{dt} \left[\int_0^\infty dx L(x) \Delta h(t - x) \right]. \quad (10)$$

In the above equation, the second term on the right is simply a convolution of the postsynaptic potential Δh with a noise-dependent filter L . If there is no noise and the slope of the membrane trajectory u' is constant between spikes, this term reduces to $A_0 \frac{d}{dt} PSP(t) / u'$.

For our noise model and neuron, the filter is $L(x) = L_1(x) + L_2(x) \cdot \frac{d}{dt}$, where

$$\begin{aligned} L_1(x) &= \int_x^\infty \frac{\partial f}{\partial u} [u_0(\hat{x} - x); u'_0(\hat{x} - x)] S_0(\hat{x}) d\hat{x} \\ &\quad - S_0(x) \int_0^x e^{-\frac{x}{\tau_m}} \frac{\partial f}{\partial u} [u_0(\hat{x} - x); u'_0(\hat{x} - x)] d\hat{x} \\ L_2(x) &= \int_x^\infty \frac{\partial f}{\partial u'} [u_0(\hat{x} - x); u'_0(\hat{x} - x)] S_0(\hat{x}) d\hat{x} \\ &\quad - S_0(x) \int_0^x e^{-\frac{x}{\tau_m}} \frac{\partial f}{\partial u'} [u_0(\hat{x} - x); \\ &\quad u'_0(\hat{x} - x)] d\hat{x}. \end{aligned} \quad (11)$$

Here $u_0(t - \hat{t})$ is the unperturbed membrane potential and S_0 is the unperturbed survivor function defined above.

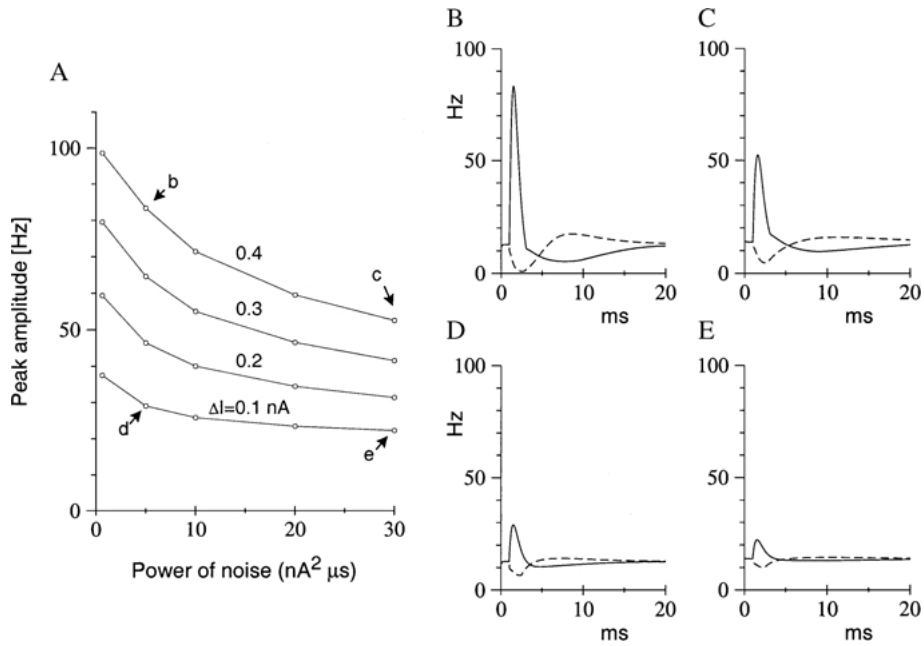


Figure 7. **A:** PSTH peak amplitudes as a function of noise level, for alpha-shaped input pulses (rise time 0.5 ms) at $t = 0$, with different positive input pulse amplitudes $|\Delta I|$. The predicted PSTHs corresponding to the four indicated points *b*, *c*, *d*, *e* are shown in the plots at right (**B–E**) (solid lines). Also shown in the plots at right are the predicted responses for negative pulses of the same amplitude (dashed); the responses are highly unsymmetric (not shown in the left-hand plot). The PSTHs were calculated by numerically integrating Eq. (9) using the full model with escape noise as indicated in the text.

The integrals in Eq. (11) may be evaluated numerically. The derivatives $\partial f/\partial u$ and $\partial f/\partial u'$ are obtained from the definition of the escape rate $f(u - \vartheta)$, and S_0 is also calculated from the escape rate. These filters have the same form as those obtained for the standard integrate-and-fire neuron in Herrmann and Gerstner (2000); the difference is that the membrane potential u is calculated using the new kernels, Eqs. (3) and (4).

3.2. Simulations

We performed simulations of model neurons subjected to stochastic background input (diffusive noise) using the parameters in Table 1. Figure 2 shows simulated PSTHs obtained using the model with the parameters specified above, and inputs and noise levels similar to those applied to rat hypoglossal motoneurons in the experiments of Poliakov et al. (1996). The simulations produce PSTHs that are qualitatively similar to the experiments, especially considering the ad hoc nature of the parameter values and kernels we used. As in the experiments of Poliakov et al. (1996), applying $30 \text{ nA}^2 \mu\text{s}$ reduces the low-noise peak amplitude by about half; the following trough is also reduced.

To evaluate the linear approximation for the escape noise model (Eq. (10)), we calculated the filters and used them to predict the PSTH responses of model neurons to the same inputs and noise conditions as for the simulations. These are also shown in Fig. 2, along with responses predicted using the full nonlinear model Eq. (9). Compared to the full model, the linear approximation overestimates the peak amplitude somewhat for these parameters. This is consistent with the results obtained above threshold in the companion article for the standard integrate-and-fire model.

Figure 7 shows theoretically calculated PSTH amplitudes as a function of noise level and input amplitude, for a range of inputs and noise levels including those used in the experiments of Poliakov et al. (1996). The results are in good qualitative agreement with their findings (see Poliakov et al., 1996, Fig. 3(c)).

Finally, we investigated how noise affects responsiveness to sub-threshold impulses in our model by measuring PSTH peak amplitudes predicted using our theory, again for a range of inputs and noise levels that includes those used in the experiments of Poliakov et al. (1996). In the companion paper, we had found that for the integrate-and-fire model, the highest response

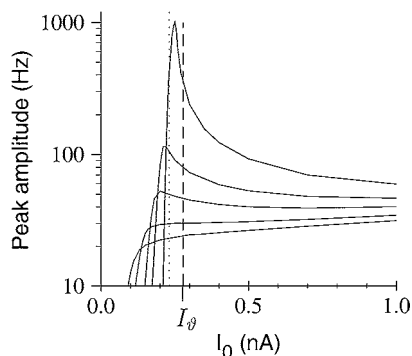


Figure 8. PSTH peak amplitudes as a function of baseline input current I_0 for alpha-shaped input pulses of amplitude 0.2 nA (rise time 0.5 ms) using the same noise levels as in Fig. 7. From top to bottom, the noise levels are: $\sigma_u = 0.32$ mV, 0.9 mV, 1.28 mV, 1.8 mV, and 2.25 mV. The corresponding equivalent noise power levels for Gaussian current noise with 10 KHz bandwidth are 0.6, 5, 10, 20, and $30 \text{ nA}^2 \mu\text{s}$. The noise-free current threshold for the parameters used is $I_\theta = \vartheta/R = 0.278$ nA, indicated by the vertical dashed line. The vertical dotted line indicates the level below which no response is possible if there is no noise. Peak amplitudes were measured from theoretical PSTHs calculated by numerically integrating Eq. (9) using the full model with escape noise as indicated in the text.

amplitudes could be obtained in low noise when the mean input potential is below threshold and that adding noise can extend the range of responsiveness to sub-threshold inputs. As shown in Fig. 8, our results indicate that a similar effect occurs with the neuron model studied here. Without noise, no response can occur when the mean potential is more than one PSP amplitude below threshold; the corresponding minimum current level is indicated by the vertical dot-dashed line. With the parameters used here and for input pulses of amplitude 0.2 nA, the minimum current for a response is about $I_{\min} = 0.23$ nA. With a noise level equivalent to $30 \text{ nA}^2 \mu\text{s}$, this minimum is lowered: at 0.1 nA, when the mean firing rate is only 1.4 Hz, a 12-Hz peak amplitude is predicted.

4. Discussion

In this section, we review some findings by other researchers about the neurophysiology of motoneurons that can be understood using our model. First, we survey previous work pertaining to measurements of motoneuron response to current transients using the PSTH and relate it to our own results. After briefly summarizing experimental results establishing the principal source of noise in motoneurons, we discuss the limi-

tations and predictions of our model. A nice overview of the problems and main theoretical argument can be found in Sections 4.4 and 4.5 of Abeles (1991).

4.1. Estimates of the Motoneuron Input-Output Transform $P(\text{spike})$

The PSTH is used in physiological experiments to estimate the motoneuron input-output transform—i.e., the firing probability in response to a stimulus, $P(\text{spike})$ (Moore et al., 1966). If the stimulus is a presynaptic spike, the measurement is called a *cross-correlogram*. It has been used extensively (Fetz and Gustafsson, 1983; Kirkwood and Sears, 1978; Knox, 1974; Moore et al., 1970; Poliakov et al., 1997; Poliakov et al., 1996) to document the input-output transform of motoneurons. The characteristics of the background noise can be as important as the PSP shape itself (Kirkwood and Sears, 1979), which has implications for the interpretation of the form of the PSTH or cross-correlogram; the amount of noisy background input must be taken into account when making comparisons (Kirkwood and Sears, 1991).

Early physiological studies of motoneuron responses seemed to indicate that the shape of the PSTH response to a presynaptic pulse resembled the PSP, to the extent that it was possible to actually measure the PSP (Moore et al., 1970, in *Aplysia*; Lindsley and Gerstein, 1979, in crayfish claw motoneurons). Moore et al. (1970) argued that to first approximation, this type of PSP-like response was to be expected given a firing rate inversely proportional to the distance between the potential and the threshold. Note that their intuitive ideas are consistent with the threshold-based escape noise models discussed in this article in the subthreshold regime. Our theory predicts the same results in the limit of high noise. Moore et al. (1970) predicted that additional secondary peaks would appear if the postsynaptic cell was firing regularly, as we also find in our theory.

Subsequently, Knox (1974) calculated the distribution of the membrane potential for a leaky integrator without noise or refractoriness, with a single presynaptic input consisting of a stationary Poisson train of identical, exponentially decaying PSPs. He found that $P(\text{spike})$ in this case would be proportional to the temporal derivative of the PSP; see Abeles (1991) for a review of the argument. Our theory predicts the same behavior in the low-noise limit. Knox's model, however, holds only for low output rates (when refractoriness can be neglected).

Combining these two views, Kirkwood and Sears (1978) proposed that $P(\text{spike})$ be a linear combination of the PSP and the PSP derivative. They found results consistent with this model in intercostal muscle afferents and ventral root afferents during respiration, but were limited to using excitatory PSPs (EPSPs) recorded in separate experiments. Fetz and Gustafsson (1983) were able to record the PSPs simultaneously with the action potential response of cat motoneurons. They found that while the linear combination can describe the appearance of the PSTH under some conditions, in which case the PSP derivative dominates the response, synaptic noise affects the relative contributions of the two components and that the inhibitory PSP (IPSP) response is not well described. They analyzed a noiseless threshold-crossing model of the tonically firing motoneuron in which the membrane trajectory and PSP shape are approximated using linear segments. According to this model, for larger PSPs, motoneuron firing probability is proportional not only to the derivative of the PSP but also inversely to the slope of the membrane trajectory,

$$\Delta\text{PSTH} \propto \frac{\text{PSP}'}{u'} \quad (12)$$

As in the Knox model, the only noise is in the random phase of the tonically firing neuron before the stimulus. In the low-noise limit, Eq. (12) is consistent with our theory.

In experiments on cat spinal motoneurons, Gustafsson and McCrea (1984) studied smaller PSPs with various noise levels, finding support for the idea that the relative weighting of the two linear terms might be a function of the ratio of PSP amplitude to noise amplitude, with the PSP fraction increasing with noise level. Kirkwood and Sears (1991) reported the results of a calculation by H. B. Bostock in which this is also the case, for a model in which both the membrane potential and its derivative are Gaussian-distributed below threshold about a stationary mean potential \bar{u} . Bostock found that the probability of firing is, to first order in PSP and PSP':

$$P[\text{spike}] \propto \exp\left(-\frac{(\vartheta - \bar{u})^2}{2\sigma^2}\right) \times \left[\frac{(\vartheta - \bar{u})}{\sigma} \text{PSP}(t) + \frac{\pi}{2\sigma'} \text{PSP}'(t) \right],$$

where the standard deviations of the membrane potential and its derivative are σ and σ' respectively; ϑ is the

threshold. However, a required assumption in obtaining the above is that the mean distance below threshold is large compared to the amplitude of the PSP. While the structure of the formula is reminiscent of our escape rate in Eq. (7), we have not yet been able to find a situation in which our formula for the PSTH, Eq. (10), would reduce to Bostock's formula. Indeed, in a later study, Poliakov et al. (1996) noted that this model predicts peak rise and fall times much shorter than those observed, implying that the time scale of the response peak is not simply the same as that of the PSP derivative.

Midroni and Ashby (1989) performed simulations of the Fetz and Gustafsson model, using regular and then irregular "noise PSP" spacing. They proposed that the form of the PSTH peak is a combination of two terms. One term describes the response without background input,

$$\Delta\text{PSTH} \propto \begin{cases} \frac{\text{PSP}'(t)}{u'} & \text{PSP}'(t) + u' \geq 0 \\ 0 & \text{otherwise} \end{cases}, \quad (13)$$

where u' is the slope of the reference trajectory, and PSP' is the time derivative of the PSP, which is reminiscent of our results in the lownoise limit. They argue that additional background input pulses that arrive at intervals Δ_n can shift the potential across threshold, which motivates a second term of the form

$$\Delta\text{PSTH} \propto \frac{1}{\Delta_n} \text{PSP}(t), \quad (14)$$

where $1/\Delta_n$ is the "noise frequency." If the noise frequency is increased ($\Delta_n \rightarrow 0$), the term in Eq. (14) dominates over Eq. (13). Hence, the position of the peak of the PSTH should depend on the noise frequency, which does not correspond to physiological observations (Poliakov et al., 1996). As an aside we note that our escape noise model assumes white noise—i.e., there is no cutoff frequency for the noise.

Poliakov et al. (1996, 1997) applied a more complete set of current stimuli injected into the soma of both rat hypoglossal and cat lumbar motoneurons, confirming these findings and also showing that higher-order interactions (dependent on the time of the preceding spike) were also not represented in the Kirkwood and Sears proposal. In particular, the fitting coefficients of the linear-combination model cannot reproduce the full range of PSTH profiles observed for a given motoneuron at different firing rates (Poliakov et al., 1997). They then focused on a Wiener kernel description

(Poliakov et al., 1997); the first-order (linear) kernel successfully captures both the peak delay and peak/trough shape, while the second-order kernel is required to model the inhibitory response and the history dependence. However, although it produces a successful description under fixed conditions, their Wiener-kernel approach does not allow predictions to be made about the response under different noise conditions.

In a theoretical study, Poliakov (1991) analyzed a model based on a linear approximation to the membrane trajectory of the tonically firing motoneuron, with noise being added to the membrane potential *after* integration. This model predicts that increasing the noise level results in an increased time-to-peak. Later, Poliakov et al. (1996) systematically studied the effect of noise level on the response of rat and cat motoneurons and confirmed that the Fetz-Gustafsson threshold-crossing model did not adequately describe the PSTH shape under low noise conditions. The experiments showed that under low-noise conditions, the typical PSTH exhibited a peak followed by a trough of equal area; increasing the noise level reduced the size of the peak and decreased the depth of the trough following the peak, but the peak did not shift to a later time.

To summarize, a number of studies have documented the effect of noise on the shape of the PSTH response to a stimulus (which could be a presynaptic spike, a current, or a PSP). Previous models of the effect of noise on the shape of the PSTH have serious restrictions concerning the shape of the membrane potential trajectory. While some models neglect refractoriness completely (Knox, 1974; Moore et al., 1970; Gustafsson and McCrea, 1984; Kirkwood and Sears, 1991), other models (Kirkwood and Sears, 1978; Poliakov, 1991) approximated the membrane potential trajectory using a linear segment and therefore do not apply to the subthreshold mode. The model presented in this article incorporates arbitrary PSP and refractory functions, covers a continuum of noise levels, and spans the range of firing regimes from subthreshold to tonic firing.

4.2. Limitations of the Model

4.2.1. Noise Model. In our analytical model, we describe noise using an escape rate function; we have shown that by an appropriate choice of escape function we can obtain a good approximation of a noisy integration (diffusive noise) process. Our diffusive noise model simulates membrane potential fluctuations caused by background synaptic input, the main source

of noise in motoneurons: Calvin and Stevens (1968) performed intracellular recordings in cat lumbosacral motoneurons showing that synaptic input causes the membrane potential to fluctuate about an otherwise steady level with an exponentially time-filtered Gaussian distribution. The membrane potential peak-to-peak amplitude can reach several mV (Granit et al., 1966; Gustafsson and McCrea, 1984), enough to trigger occasional spikes even when the mean potential is well below threshold; in tonically firing human motoneurons, synaptic noise is known to play a major role (Matthews, 1996). It should be noted that background synaptic activity has also been found to increase conductance significantly in dendrites of neocortical pyramidal neurons (Paré et al., 1998) and in cerebellar Purkinje cells (Hausser and Clark, 1997), thus decreasing cellular responsiveness; our model does not describe these effects explicitly. Instead, we use an “effective” membrane time constant $\tau_m = 4$ ms, which is shorter than the passive time constant measured at rest (Bernander et al., 1991).

4.2.2. Voltage Trajectories. The neuron description we have used produces trajectories of the membrane potential that only approximate those of real motoneurons. We attribute the differences between the experimental PSTHs of Poliakov et al. (1996) and the simulated PSTHs of Fig. 2 mainly to the ad hoc nature of the parameter values and kernels we used. Although dynamically changing conductances have a significant cumulative effect on the threshold-crossing behavior, they are represented here only summarily. Several types of improvements to the model might be considered.

1. The simple scalar factor we adopted here only captures spike-dependent amplitude changes in the response to a pulse. However, temporal changes also occur in the pulse response because of dynamic conductances (Schwindt and Calvin, 1973; Kistler et al., 1997), suggesting that better biological realism could be obtained by adding another modulation to the membrane response kernel ε in the form of a “time constant of the time constant” that would allow τ_m to increase with $t - \hat{t}$ (Stevens and Zador, 1998). However, whatever the value of this time constant, the effect on the form of the PSTH is expected to be small because the effective time constant would not change very much over the time scale of the input pulse.
2. Additionally, it is known that the time course of the input conductance of motoneurons is different at

different drive levels, and differs from that measured during the afterhyperpolarization following a single spike (Schwindt and Calvin, 1973). Our model does not produce a drive-level dependent conductance.

3. The membrane response kernel used here is based on a decaying exponential. However, kernels of real neurons are more complex; for example, kernels of Hodgkin-Huxley type neurons exhibit oscillations (Kistler et al., 1997). An even better description using the spike response model could be obtained by deriving the kernels directly from experimental measurements in the same way as they were obtained for the Hodgkin-Huxley model by Kistler et al. (1997).

4.3. Predictions of the Model

To our knowledge, the only direct physiological measurements of the effect of noise on the PSTH response of neurons to current pulses have been in motoneurons stimulated with a suprathreshold current (Poliakov et al., 1996, 1997; Fetz and Gustafsson, 1983). Our theory allows two general predictions to be made.

First, the same effect of noise on the PSTH should be observable when the baseline current is subthreshold: in low noise, the shape of the PSTH should exhibit a trough following the main peak; as noise increases, the peak amplitude should decrease and the trough should become less pronounced. Since the firing rate is rather sensitive to noise in the subthreshold regime, the mean input I_0 may be readjusted in order to keep the firing rate constant so as to extract the effect of noise on the PSTH. A secondary peak should appear following the initial peak, at a delay corresponding to the mean interval. Secondary peaks are observed experimentally in the suprathreshold regime (e.g., Powers and Binder (1996) in cat motoneuron) but, to our knowledge, have not been reported below threshold, where they are likely to be more difficult to observe because of low firing rates.

Second, our model allows predictions to be made about the effect of changing the baseline current level. Motoneurons operate over a range of mean input levels, from the subthreshold regime Matthews (1996) to tonic firing (Calvin and Stevens, 1968). If synaptic noise were very low, our model would predict that motoneuron responses to input pulses is very strongly dependent on the mean input level: responsiveness changes dramatically as the mean input approaches threshold and the neuron switches from subthreshold mode to

tonic firing (top curve in Fig. 8). However, many studies (Calvin and Stevens, 1968; Granit et al., 1966; Gustafsson and McCrea, 1984; Matthews, 1996) have established that the level of synaptic noise in motoneurons generates a standard deviation of the membrane potential of a few mV. According to our model, at this level of noise (bottom two curves in Fig. 8), the discontinuity in responsiveness just below threshold disappears. Furthermore, at this level of noise, the range of response below threshold is extended. These predictions can be tested by measuring the PSTH peak amplitude at different baseline current levels.

5. Conclusions

We have presented a simple extension of the integrate-and-fire neuron based on the spike-response model that gives biologically plausible firing rates and membrane trajectories using typical motoneuron values of the passive membrane time constant and input resistance. Using an escape-rate approach to model diffusion noise, we have shown how the noise level controls the shape of the neuron's PSTH response to an input pulse. The model qualitatively reproduces experimentally observed noise level-dependent changes in the PSTH. We have thus demonstrated that the experimentally observed effect of noise on the form of the PSTH does not depend on properties such as adaptation or specific ionic conductances. Although the spike-response model is a highly simplified description of biological neurons, it may nevertheless be applicable when nonlinear properties of the dendrites are unimportant. In particular, it is valid for the experimental situation of current injection into the soma of electrotonically compact motoneurons. Our model shows that noise can play a significant role in signal transmission in motoneurons in the subthreshold range by extending the response range. In very low noise, extremely high responses occur in response to an input pulse when the mean input is just below threshold. Increasing the noise level makes the response to an input pulse less sharply dependent on the mean drive level. Our results may help to understand a broad set of experimental measurements (Fetz and Gustafsson, 1983; Kirkwood and Sears, 1978; Poliakov et al., 1996, 1997).

6. Appendix

To obtain $\Delta A(t)$ for our new neuron model, we must briefly return to the theory of population dynamics

(Gerstner, 2000). According to this theory, the following equation must hold:

$$0 = \frac{d}{dt} \int_{-\infty}^t S_h(t | \hat{t}) A(\hat{t}) d\hat{t}.$$

By linearizing this equation in ΔA or Δh , the following is obtained:

$$0 = \frac{d}{dt} \int_{-\infty}^t S_0(t - \hat{t}) \Delta A(\hat{t}) + A_0 \frac{d}{dt} \times \left\{ \int_{-\infty}^t dt_1 \int_{-\infty}^{t_1} d\hat{t} \Delta h(t_1 | \hat{t}) \frac{\partial S_h(t | \hat{t})}{\partial \Delta h(t_1 | \hat{t})} \Big|_{\Delta h=0} \right\}. \quad (15)$$

This expression cannot immediately be evaluated because of the dependence on \hat{t} of the potential in the second term. However, for the specific kernels defined in Section 2.2, it is easy to show that $h(t | \hat{t}) = (1 - \exp[-(t - \hat{t})/\tau_r]) (h_{\text{free}}(t) - \exp[-(t - \hat{t})/\tau_m] h_{\text{free}}(\hat{t}))$ where $h_{\text{free}}(t) \doteq \int_0^\infty \epsilon(s) I(t - s) ds$. Before the pulse, the input potential depends on the time of the last spike \hat{t} —i.e. $h_0(t | \hat{t}) = (1 - \exp[-(t - \hat{t})/\tau_r]) \Delta h_{\text{free}}(\hat{t})$; note $\Delta h_{\text{free}}(\hat{t}) = (\tau_m/\tau_r) R I_0$. Application of the pulse $\Delta I(t)$ causes a fluctuation

$$\Delta h(t | \hat{t}) = (1 - e^{-\frac{(t-\hat{t})}{\tau_r}}) (\Delta h_{\text{free}}(t) - \Delta h_{\text{free}}(\hat{t}) e^{-\frac{(t-\hat{t})}{\tau_m}}). \quad (16)$$

Therefore, $\partial \Delta h(t | \hat{t}) / \partial \Delta h_{\text{free}}(t) = (1 - e^{-\frac{(t-\hat{t})}{\tau_r}})$ and so

$$\frac{\partial S_h(t | \hat{t})}{\partial \Delta h(t_1 | \hat{t})} = (1 - e^{-\frac{(t-\hat{t})}{\tau_r}})^{-1} \frac{\partial S_h(t | \hat{t})}{\partial \Delta h_{\text{free}}(t_1)}. \quad (17)$$

When Eqs. (16) and (17) are used in Eq. (15), the dependence of the potential on \hat{t} is removed. Rearrangement gives Eq. (10) with the filters of Eq. (11).

Notes

1. For infinitely short current pulses $I(t) = q\delta(t - t_0)$, the response amplitude would be independent of the conductance, depending only on the membrane capacity and the charge q . Below we focus (as in the case of Poliakov et al., 1996) on current pulses $I(t) = q(t/\tau_s^2) \exp(-t/\tau_s)$ of finite width τ_s . In this case the response amplitude does depend on the conductance and so on the time $t - \hat{t}$ since the last output spike. This dependence is mimicked by Eq. (4).
2. The time constant in the refractory function is changed to τ_{refr} , and the update rule for h in step 5a is changed to $h(\Delta_j) = h_{\text{free}}(t) [1 - \exp(-\Delta_j/\tau_{\text{rec}})]$.

References

- Abeles M (1991) *Corticonics*. Cambridge University Press, Cambridge.
- Bernander Ö, Douglas RJ, Martin KA, Koch C (1991) Synaptic background activity influences spatiotemporal integration in single pyramidal cells. *Proc. Natl. Acad. Sci. USA* 88: 11569–11573.
- Calvin WH, Stevens CF (1968) Synaptic noise and other sources of randomness in motoneurone interspike intervals. *J. Neurophysiol.* 31: 574–587.
- Cox DR (1962) *Renewal Theory*. Methuen, London.
- Paré D, Shink E, Gaudreau H, Destexhe A, Lang EJ (1998) Impact of spontaneous synaptic activity on the resting properties of cat neocortical neurons in vivo. *J. Neurophysiol.* 79: 1450–1460.
- Fetz EE, Gustafsson B (1983) Relation between shapes of post-synaptic potentials and changes in firing probability of cat motoneurons. *J. Physiol.* 341: 387–410.
- Gerstner W (1995) Time structure of the activity in neural network models. *Phys. Rev. E.* 51(1): 738–758.
- Gerstner W (2001) A framework for spiking neuron models: The spike response method (Preprint). In: Gielen S, et al., eds. *The Handbook of Biological Physics* Elsevier, Amsterdam, pp. 469–516. Available at <http://diwww.epfl.ch/lami/team/gerstner/>.
- Gerstner W (2000) Population dynamics of spiking neurons: Fast transients, asynchronous states and locking. *Neural Comput.* 12: 1–46.
- Granit R, Kernell D, Lamarre Y (1966) Algebraic summation in synaptic activation of motoneurons firing within the ‘primary range’ to injected currents. *J. Physiol.* 187: 379–399.
- Gustafsson B, McCrea D (1984) Influence of stretch-evoked synaptic potentials on firing probability of cat spinal motoneurons. *J. Physiol.* 347: 431–451.
- Hausser M, Clark BA (1997) Tonic synaptic inhibition modulates neuronal output pattern and spatiotemporal synaptic integration. *Neuron.* 19: 665–678.
- Herrmann AK, Gerstner W (2000) Noise and the PSTH response to current transients: I. General theory and application to the integrate-and-fire neuron. *J. Comp. Neurosci.*
- Jones KE, Bawa P (1999) A comparison of human motoneuron data to simulated data using cat motoneuron models. *J. Physiol. Paris* 93(1–2): 43–59.
- Kirkwood PA (1979) On the use and interpretation of cross-correlation measurements in the mammalian central nervous system. *J. Neurosci. Methods* 1: 107–132.
- Kirkwood PA, Sears TA (1978) The synaptic connexions to intercostal motoneurons as revealed by the average common excitation potential. *J. Physiol.* 275: 103–134.
- Kirkwood PA, Sears TA (1991) Cross-correlation analysis of motoneurone inputs in a co-ordinated motor act. In: Krüger J, ed. *Neuronal Co-operativity*. Springer-Verlag, Berlin. pp. 225–248.
- Kistler WM, Gerstner W, van Hemmen JL (1997) Reduction of Hodgkin-Huxley equations to a single-variable threshold model. *Neural Comput.* 9: 1015–1045.
- Knox CK (1974) Cross-correlation functions for a neuronal model. *Biophys. J.* 14: 567–582.
- Lindsley BG, Gerstein GL (1979) Interactions among an ensemble of chordotonal organ receptors and motor neurons of the crayfish claw. *J. Neurophysiol.* 42: 383–399.

- Matthews PBC (1996) Relationship of firing intervals of human motor units to the trajectory of post-spike after-polarization and synaptic noise. *J. Physiol.* 492.2: 597–628.
- Midroni G, Ashby P (1989) How synaptic noise may affect cross-correlations. *J. Neurosci. Meth.* 27: 1–12.
- Moore GP, Perkel DH, Segundo JP (1966) Statistical analysis and functional interpretation of neuronal spike data. *Ann. Rev. Physiol.* 28: 493–522.
- Moore GP, Segundo JP, Perkel DH, Levitan H (1970) Statistical signs of synaptic interaction in neurons. *Biophys. J.* 10: 876–900.
- Paré D, Shink E, Gaudreau H, Destexhe A, Lang E (1998) Impact of spontaneous synaptic activity on the resting properties of cat neocortical neurons in vivo. *J. Neurophysiol.* 79: 1450–1460.
- Perkel DH, Gerstein GL, Moore GP (1967) Neuronal spike trains and stochastic point processes I. The single spike train. *Biophys. J.* 7: 391–418.
- Piotrkiewicz M, Churikova L, Person R (1992) Excitability of single firing human motoneurons to single and repetitive stimulation (experiment and model). *Biol. Cybern.* 66(3): 253–259.
- Plesser HE, Gerstner W (2000) Noise in integrate-and-fire neurons: From stochastic input to escape rates. *Neural Comput.* 12: 367–384.
- Poliakov AV (1991) Synaptic noise and the cross-correlation between motoneuron discharges and stimuli *Neuro Report* 2: 489–492.
- Poliakov AV, Powers RK, Binder MD (1997) Functional identification of the input-output transforms of motoneurons in the rat and cat. *J. Physiol.* 504 (Pt. 2): 401–424.
- Poliakov AV, Powers RK, Sawczuk A, Binder MD (1996) Effects of background noise on the response of rat and cat motoneurons to excitatory current transients. *J. Physiol.* 495 (Pt. 1): 143–157.
- Powers RK, Binder MD (1996) Experimental evaluation of input-output models of motoneuron discharge. *J. Neurophysiol.* 75: 367–379.
- Schwindt PC, Calvin WH (1973) Nature of conductances underlying rhythmic firing in cat spinal motoneurons. *J. Neurophysiol.* 36: 955–973.
- Stevens CF, Zador AM (1998) Novel integrate-and-fire-like model of repetitive firing in cortical neurons. In: *Proceedings of the Fifth Joint Symposium on Neural Computation*, UCSD, La Jolla, CA. Available at http://www.sloan.salk.edu/~zador/rep_fire_inc/rep_fire_inc.html.